Effect of randomness and anisotropy on Turing patterns in reaction-diffusion systems

Indrani Bose and Indranath Chaudhuri
Department of Physics,
Bose Institute,
93/1, Acharya Prafulla Chandra Road,
Calcutta-700 009, India.

Abstract

We study the effect of randomness and anisotropy on Turing patterns in reaction-diffusion systems. For this purpose, the Gierer-Meinhardt model of pattern formation is considered. The cases we study are: (i)randomness in the underlying lattice structure, (ii)the case in which there is a probablity p that at a lattice site both reaction and diffusion occur, otherwise there is only diffusion and lastly, the effect of (iii)anisotropic and(iv)random diffusion coefficients on the formation of Turing patterns. The general conclusion is that the Turing mechanism of pattern formation is fairly robust in the presence of randomness and anisotropy.

PACS Numbers: 05.70 Ln

I. Introduction

In 1952 Turing [1] pointed out that diffusion need not always act to smooth out concentration differences in a chemical system. Two interacting chemicals can generate a stable, inhomogeneous pattern if one of the substances(the inhibitor) diffuses much faster than the other(the activator). The activator is autocatalytic, i.e, a small increase in its concentration 'a' over its homogeneous steady-state concentration leads to a further increse of 'a'. The activator besides promoting its own production also promotes the production of the inhibitor. The inhibitor, as the name implies, is antagonistic to the activator and inhibits its production. Suppose, originally the system is in a homogeneous steady state. A local increase in the activator concentration

leads to a further increase in the concentration of the activator due to autocatalysis. The concentration of the inhibitor is also increased locally. The inhibitor, having a diffusion coefficient much larger than that of the activator, diffuses faster to the surrounding region and prevents the activator from coming there. This process of autocatalysis and long-rang inhibition finally lead to a stationary state consisting of islands of high activator concentration within a region of high inhibitor concentration. The islands constitute what is known as the Turing pattern. Turing's original idea was that the stable patterns could be linked to the patterns seen in biological systems. Experimental evidence of Turing patterns, however, came much later and that too not in biological systems but in chemical systems [2, 3, 4]. This has sparked renewed interest in mathematical models of pattern formation as well as the relationship of chemical patterns to the remarkably similar patterns observed in diverse physical and biological systems [5]. Turing structures have also been seen in electrical gas discharge systems [6]. Recently, it has been suggested that the formation of stripe patterns on the marine angelfish Pomacanthus can be explained on the basis of Turing mechanism involving reaction-diffusion(RD) [7]. A RD neural network model has been proposed based on nonsynaptic diffusion neurotransmission [8]. The model has the features of short-range activation and long-rang inhibition, necessary ingredients for the formation of Turing patterns. The network exhibits similar self-organization behaviour.

The diverse examples mentioned above show that the Turing patterns are not unique to a particular system. Also Turing mechanism embodies a general principle of self-organization. A well-known model of a RD system in which Turing patterns can form is the Gierer-Meinhardt(GM) model [9, 10]. In Section II, we describe the GM model and study the effect of randomness in the structure of the RD system on the pattern formation process(Case I). For this purpose the differential equations of the model are discretized on a square lattice. We further study the situation in which there is a probability p that at a lattice site both reaction and diffusion occur, otherwise there is only diffusion(Case II). In Section III, we study the effect of anisotropic and random diffusion coefficients(Case III and Case IV) on the formation of Turing patterns. All the studies are based on computer simulation on a squre lattice. Section IV contains a general discussion of the models studied.

II. Randomness in structure and dynamics

The differential equations describing RD in the GM model are

$$\frac{\partial a}{\partial t} = D_a \Delta a + \rho_a \frac{a^2}{h} - \mu_a a \qquad (1a)$$
$$\frac{\partial h}{\partial t} = D_h \Delta h + \rho_h a^2 - \mu_h h \qquad (1b)$$

where Δ is the Laplacian given by $\Delta = \frac{\partial^2}{\partial x^2} + \frac{\partial^2}{\partial y^2}$, 'a' and 'h' denote the concentrations of the activator and the inhibitor, D_a, D_h, are the respective diffusion coefficients, μ_a, μ_h are the removal rates and ρ_a, ρ_h are the cross-reaction coefficients. The conditions for the formation of stable Turing patterns are $D_h >> D_a$ and $\mu_h > \mu_a$ [10]. We also assume that $\rho_a = \mu_a$ and $\rho_h = \mu_h$. In this case, the steady state solution of equations (1a) and (1b) is given by (a,h)=(1,1), i.e., the steady state is homogeneous. The homogeneous steady state is stable if local fluctuations created in the system decay with time. If the fluctuations grow with time, the original homogeneous state is unstable. A phase diagram ($\mu = \frac{\mu_h}{\mu_a}$ versus $D = \frac{D_a}{D_h}$), based on the linear stability analysis, of the one-dimensional(1d) version of the GM model is given in Ref.[10]. The phase diagram contains a region in which Turing patterns can form. In this parameter regime, instability in the original homogeneous state leads finally to a steady state in which Turing patterns of high activator concentration are formed. Appendix B of the same Ref.[10] gives the parameter values for a two-dimensional(2d) RD system for which Turing patterns can form in the steady state. We use these parameter values, $D_a = 0.005$, $\rho_a = \mu_a = 0.01$ and $D_h = 0.2$, $\rho_h = \mu_h = 0.02$, for our studies.

As in [10] a very simple discretization scheme is used. The Laplacian Δ applied to the function a(x,t) is taken as

$$\Delta a(x_{ij}, t) = \frac{a(x_{i+1j}, t) + a(x_{ij+1}, t) + a(x_{i-1j}, t) + a(x_{ij-1}, t) - 4a(x_{ij}, t)}{\delta x^2} \qquad (2)$$

where x_{ij} denotes a lattice site, $x_{ij} = (i\delta x, j\delta x)$. Time is also discretized, $t_k = k\delta t$, and the time derivative approximated as

$$\frac{\partial a(x, t_k)}{\partial t} = \frac{a(x, t_{k+1}) - a(x, t_k)}{\delta t} \qquad (3)$$

In all our simulations, we choose $\delta x = \delta t = 1$. The lattice chosen is of size 30×30. Also, periodic boundary conditions are assumed.

We first study the RD process on inhomogeneous substrata(CaseI). In our case these are the (2d) percolation clusters, with site occuption probability p, on which the activator and inhibitor react and dffuse. The percolation clusters are generated in the usual manner with the help of a random number generator. If the random number is less than or equal to p, the site of the lattice is occupied, otherwise it is kept empty. All the sites of the square lattice are examined successively and the occupation status of a site determined with the help of the random number generator. The nearest-neighbour(n.n.) occupied sites constitute a percolation cluster.

The differential equations (1a) and (1b) are discretized according to the schemes specified in equations (2) and (3). The Laplacian in (2) is now written as

$$\begin{aligned} \Delta\, a(x_{ij},\, t) &= iocc(i+1,\, j) \times (\, a(x_{i+1j},\, t) - a(x_{ij},\, t)\,) \\ &+ iocc(i,\, j+1) \times (\, a(x_{ij+1},\, t) - a(x_{ij},\, t)\,) \\ &+ iocc(i-1,\, j) \times (\, a(x_{i-1j},\, t) - a(x_{ij},\, t)\,) \\ &+ iocc(i,\, j-1) \times (a(x_{ij-1},\, t) - a(x_{ij},\, t)\,) \qquad (4) \end{aligned}$$

The array iocc keeps track of the occupation status of the sites of the square lattice. If the site x_{ij} is occupied then iocc(i,j)=1, otherwise it is equal to zero. Equation(4) expresses the fact that diffusion to a site from a neighbouring site takes place only if the neighbouring site belongs to the RD network, i.e., to a percolation cluster. One can easily check that the discretized differential equations (with $\rho_a = \mu_a$ and $\rho_h = \mu_h$) have a steady state solution given by a=1 and h=1 for all the cluster sites. Random fluctuations of magnitude less than 0.1 are created in the steady state with the help of the random number generator. This fixes the values of a and h at all the cluster sites at time t=0. The values of a and h at time t+1 are determined at a site x_{ij} belonging to a cluster with the help of the discrete equations for a and h. This process is repeated till the steady state is reached, i.e., the values of a and h at all the cluster sites do not change within a specified accuracy.

We define an 'activated' zone as an island of n.n. sites in the steady state, at each of which the activator concentration has a value greater than 1 which is the homogeneous steady state value. Figs. 1(a)-1(d) show the concentration profiles in the activated zones for site occupation probabilities

p=0.9, 0.7, 0.59, and 0.4 respectively. The value $p = p_c = 0.59$ is the site percolation threshold for a square lattice. For $p > p_c$, a connected network of sites spans the lattice, for $p < p_c$, there is no spanning cluster. For $p > p_c$, the percolation clusters include both the spanning cluster as well as isolated clusters in other parts of the lattice. For $p < p_c$, the percolation clusters consist of only the isolated clusters.

The Figures show that the number of activated zones increases as p decreases. This trend continues below the percolation threshold. Also, the average height of the concentration peaks decreses. These results can be understood in the following manner. With lesser connections in the RD network, as p decreses, the inhibitor cannot diffuse to long distances and so cannot prevent activator growth in the local regions. Thus in the steady state there is a larger number of activated zones. The average height of activator-concentration profiles decreases because of the inability of the inhibitor to totally diffuse away from the activator zone. The greater concentration of inhibitor in this zone limits the growth of the activator concentration more than in the case of a regular RD network.

We next consider CaseII. In this case, the RD network is a fully connected square lattice. Let p be the probablity that both reaction and diffusion occur at a site. The other possibility, with probablity (1-p), is ordinary diffusion. When p=1, i.e., there is no randomness in the dynamics, Turing patterns form in the steady state. When p=0, i.e., there is no reaction, simple diffusion takes over. The steady state in this case is homogeneous with all concentration gradients removed. Figs. 2(a)-2(d) show the steady state patterns for p=0.01, 0.05, 0.3 and 0.7 . For p=0.005, the steady state is homogeneous. Thus for p as small as 0.01, i.e., when RD occurs at only 1% of the lattice sites a Turing pattern is formed. In this case, there is only one activated zone which covers a large area. As p increses, the number of activated zones increses. For small values of p, we have checked that an activated zone need not be centred around a cluster of n.n. sites at which RD occurs, a zone may form in the intermediate region of two such clusters. In the light of this fact, it is interesting to note that even with very few RD sites, the Turing mechanism is operative.

III. Anisotropy and randomness in diffusion coefficients

Anisotropy in the RD medium is reflected in the anisotropy of the diffusion coefficients. Mertens et al [11] have studied the effect of anisotropic diffusion coefficients on pattern formation in catalytic surface reactions. Their conclusion is that anisotropy may give rise to new types of patterns. In our Case III, we assume that for diffusion in the vertical direction, the diffusion coefficients are $D_a = 0.005$ and $D_h = 0.2$. These are the values for which Turing patterns can form in an isotropic medium. For diffusion in the horizontal direction, the diffusion coefficients D_{a1} and D_{h1} may have different values. Figs. 3(a)-3(c) show the steady state patterns for the cases (i) $D_{a1} = 0.005$, $D_{h1} = 0.01$, (ii) $D_{a1} = 0.2$, $D_{h1} = 0.005$ and (iii) $D_{a1} = 0.008$, $D_{h1} = 0.2$. In the first two cases, the stationary pattern has a wave-like appearance. This Turing pattern is different from the one consisting of islands that we have been considering so far. For a (1d) RD system, the values of diffusion coefficients given in (i) and (ii) correspond to the situation when the final steady state is homogeneous [10]. This fact is reflected in the patterns seen in Figs. 3(a) and 3(b), the distribution of the activator concentration is homogeneous in the horizontal direction. In the third case, the diffusion coefficients are such that Turing patterns are formed in the steady state. Fig.3(c) shows the usual Turing pattern consisting of islands. Thus with an appropriate choice of diffusion coefficients, one may generate different types of Turing patterns.

Case IV considers the situation of random diffusion coefficients. The diffusion coefficient D_{ij} for diffusion between a pair of sites is chosen from a binary distribution. The diffusion coefficients for the activator and the inhibitor are 0.005 and 0.2 respectively with a probablity p. The diffusion coefficients have equal values, 0.005, with probablity (1-p). The diffusion term is now discretized as

$$D_a \triangle a = \sum_j D_{\mathbf{ajk}} [\, a(j, t) - a(k, t) \,] \qquad (5)$$

where k denotes the lattice site x_{ij} and j denotes the four n.n. sites. When all the $D_{\mathbf{ajk}}$'s are equal to D_a, the original discretization is recovered. Figs.

4(a)-4(b) show the steady state patterns for $p = 0.5,\ 0.3\, and\, 0.2$ respectively. In Fig. 4(a), the Turing activator-concentration peaks are above the steady state value of 1. Figs. 4(b) shows that Turing patterns are still formed but the peaks are above or below the value 2. This implies that there is an overall activation at all the lattice sites. This is an interesting feature of the model considered. Fig. 4(c) shows that at $p = 0.2$, the steady state is homogeneous but has a higher concentration (a,h) = (2,2) than in the original steady state for which (a,h) = (1,1). The transition from a steady state with Turing patterns to a new homogeneous steady state is analogous to a dynamical phase transition and occurs at a value of p in between $p = 0.2$ and $p = 0.3$.

IV. Discussion

In Case I, we have studied pattern formation in a square network with missing connections. In chemical RD systems which exhibit Turing patterns, the RD process takes place in a gel which consists of an irregularly-connected network of pores of various diameters through which the molecules diffuse. RD processes in the brain also occur in an irregular network. The present study shows that disorder in the underlying network has no adverse effect on the formation of Turing patterns. This is because the length scales involved in the RD process are small.

In our model we have considered random n.n. connectivity. In a more general context, when further-neighbour connections are also present, an interesting problem to study is the effect of network connectivity on the stability of the dynamical system. When small perturbations are applied to a steady state, the stability of this state may be studied by linear stability analysis, i.e., by Taylor-expanding in the neighbourhood of the steady state. Only the first two terms in the expansion are kept, the second term contains the derivative or Jacobian matrix. The original steady state is stable only if all the eigenvalues of the Jacobian matrix have negative real parts. Consider a randomly-assembled dynamical network. Full connectance implies that an element of the network is connected to all the other elements. For random connectivity, the Jacobian matrix has random elements. For such a Jacobian matrix of zero mean, The Wigner-May Theorem [12, 13] states that the dynamical system is almost surely unstable if the connectivity exceeds a threshold. Raghavachari and Glazier [14] have considered 1d coupled map

lattices with a scaling form of connectivity. Each pair of sites i and j are connected with the probablity

$$p_{ij} \quad = \quad \frac{1}{|\vec{r}_i \, - \, \vec{r}_j|^{\alpha}} \, , \quad j \, = \pm 1, \, 2, \, 3, \, ... \qquad (6)$$

Where $\vec{r}_i$ and $\vec{r}_j$ are the coordinates of the ith and jth sites, respectively. The n.n. coupling limit corresponds to $\alpha \rightarrow \infty$ and $\alpha \rightarrow 0$ is the global coupling limit. For this model, the Jacobian matrix has all non-negative elements and is unstable for low values of connectivity but is stable when connectivity exceeds a critical value. In the light of these studies, it is of interest to include further-neighbour connections in the model studied in Case I and study the effect of the richer connectivity on the formation of Turing patterns. For this purpose, a discretization scheme involving an extended neighbourhood can be used. Further-neighbour connectivity may be important in neural networks in which RD prosses are responsible for self-organization in the neural activity [8].

In Case II, the model studied involves random dynamics. A possible realization of this situation is as follows. Autocatalysis of the activator may require the presence of a chemical molecule or some triggering mechanism not available at all the lattice sites. The chemical molecule in question can be static with diffusion coefficient zero because of a large size. The situation is hypothetical but not unrealistic.

In Case III and Case IV, we have studied models with anisotropic and random diffusion coefficients. In ordinary diffusion, molecules move from regions of greater to regions of less concentration at a rate proportional to the gradient of the concentration and also proportional to the diffusivity of the substance. Normally, the diffusivities are inversely proportional to the square roots of the molecular weights. However in a porous medium with tortuous geometry, the diffusion coefficients may be space dependent. The pores of the cell-walls in a biological system restrict the movement of large molecules in addition to that imposed by their weights and most of them are unable to pass through the walls of the cell. In aqueous solution, the activator and inhibitor molecules may have the same diffusion coefficients but if the RD system is embedded in a gel as in the experiments [2, 4] to observe Turing patterns, the activator molecules being larger in size are effectively trapped. This provides a big difference in diffusion coefficients of activator and inhibitor. In these examples, the diffusion coefficient is determined by

the geometrical structure of the RD medium. In a porous medium with pore sizes distributed over a range, the diffusion coefficient may very well be space-dependent.

Recent experimental evidence of Turing patterns in physical, chemical and biological systems has given rise to renewed interest in the study of these patterns. In this paper, we have considered the effect of randomness and anisotropy on the pattern formation process. The studies have been based on computer simulation and the results obtained show that the Turing mechanism of pattern formation is fairly robust in the presence of randomness and anisotropy.

Acknowledgement

The Authors thank Sitabhra Sinha and Asimkumar Ghosh for computational help. One of the Authors (IC) is supported by the Council of Scientific and Industrial Research, India under sanction No9/15(173)/96-EMR-I.

Figure Captions

Fig.1 Concentration profiles of the activator on a disordered lattice structure for site occuption probablities (a) p = 0.9, (b) p = 0.7, (c) p = 0.59 and (d) p = 0.4 (Case I). The islands of high activator concentration constitute the Turing pattern.

Fig.2 Turing patterns('a' denotes the activator concentration) for (a) p = 0.01, (b) p = 0.05, (c) p =0.3 and (d) p = 0.7 (Case II), where p is the probablity that at a lattice site both reaction and diffusion occur and (1-p) the probablity that there is only diffusion. The size of the lattice is 30×30 .

Fig.3 Steady-state patterns in the case of anisotropic diffusion coefficients (Case III). For diffusion in the vertical direction, the diffusion coefficients of the activator and inhibitor are: $D_a = 0.005 \, and \, D_h = 0.2$. For diffusion in the horizontal direction, the diffusion coefficients of the activator and inhibitor are: (a) $D_{a1} = 0.005$, $D_{h1} = 0.01$ (b) $D_{a1} = 0.2$, $D_{h1} = 0.005$ and (c) $D_{a1} = 0.008$, $D_{h1} = 0.2$.

Fig.4 Steady-state pattern for random diffusion coefficients (Case IV). The diffusion coefficients of the activator and inhibitor are 0.005 and 0.2, respectively, with a probablity p. The diffusion coefficients have equal values, 0.005, with probablity (1-p). The values of p that have been considered are: (a) p = 0.5, (b) p = 0.3 and (c) p = 0.2 .

References

[1] A.M.Turing, Phil.Trans.R.Soc.B 327, 37 (1952)

[2] V.Castets, E.Dulos, J.Boissonade and P.De Kepper, Phys.Rev.Lett. 64, 2953 (1990)

[3] Q. Ouyang and H.L. Swinney, Nature 352, 610 (1991)

[4] K.J.Lee, W. D. McCormick, Z. Noszticzius and H. L. Swinney, J. Chem. Phys. 96, 4048 (1992)

[5] M.C.Cross and P.C.Hohenberg, Rev.Mod.Phys. 65, 851 (1993)

[6] Y.Astrov, E.Ammelt, S.Teperick and H.G.Purwins, Phys.Lett. A, 211 (1996)

[7] S.Kondo and R.Asai, Nature 376, 765 (1995)

[8] P.Liang, Phys.Rev.Lett. 75, 1863 (1995)

[9] A.Gierer and H.Meinhardt, Kybernetik 12, 30 (1972)

[10] A.J.Koch and H.Meinhardt, Rev.Mod.Phys. 66, 1481 (1994)

[11] F.Mertens, N.Gottschalk, M.Bar, M.Eiswirth and A.Mikhailov, Phys.Rev.E 51, R 5193 (1995)

[12] E.P.Wigner, in Proceedings of the Fourth Canadian Mathematical Congress, edited by M.S.MacPhail (University of Toronto Press, Toronto, (1959)

[13] R.M.May, Nature 238, 413 (1972)

[14] S.Raghavachari and J.A.Glazier, Phys.Rev.Lett. 74, 3297 (1995)

Fig. 1(a)

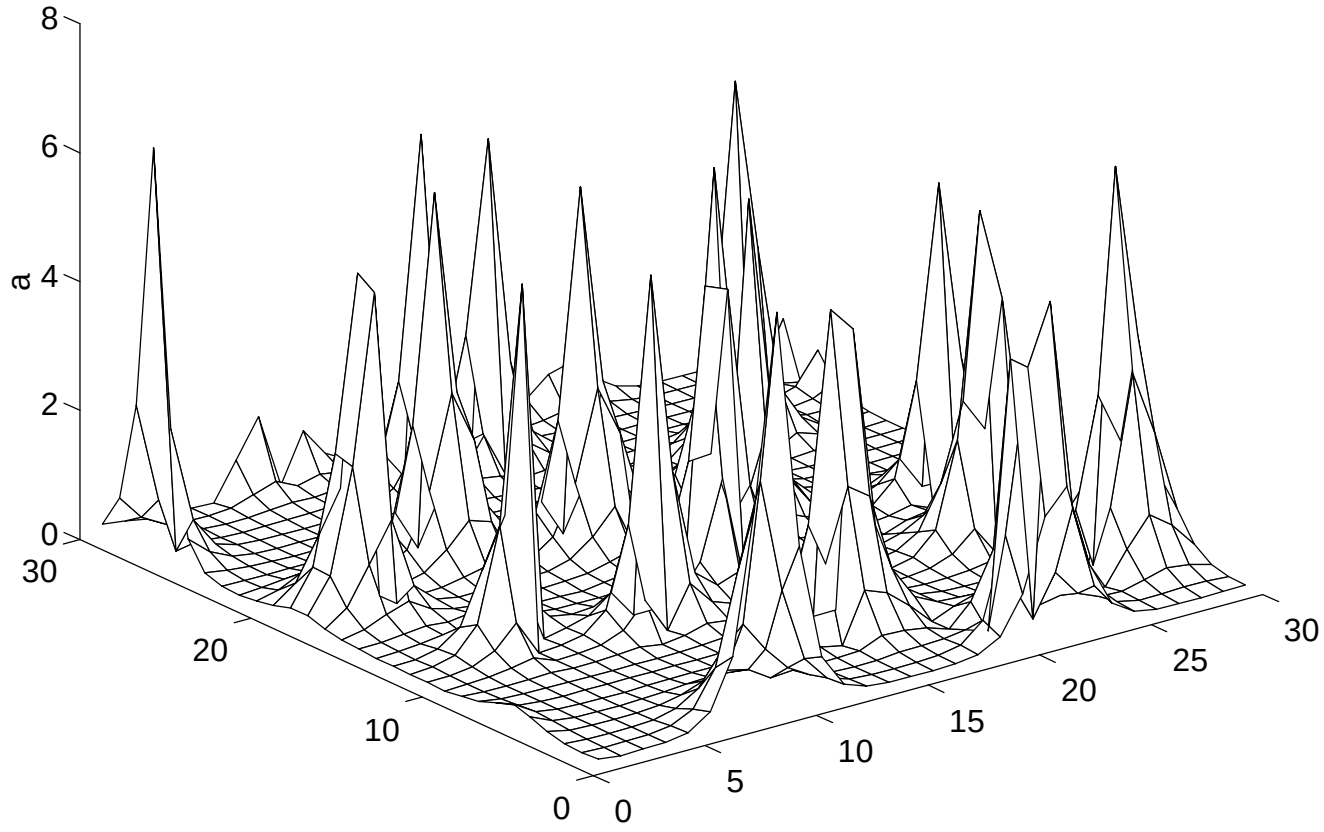

Fig. 1(b)

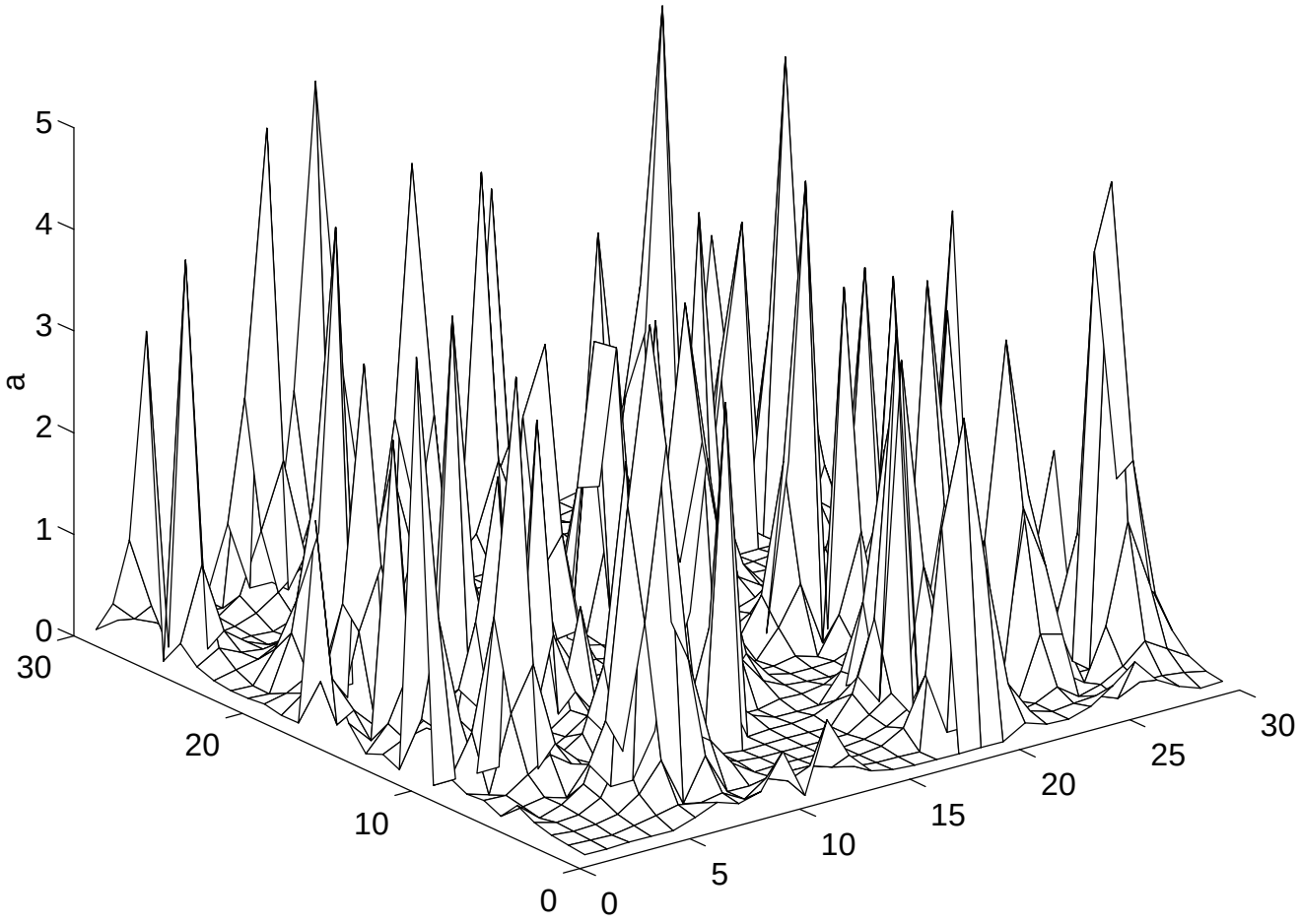

Fig. 1(c)

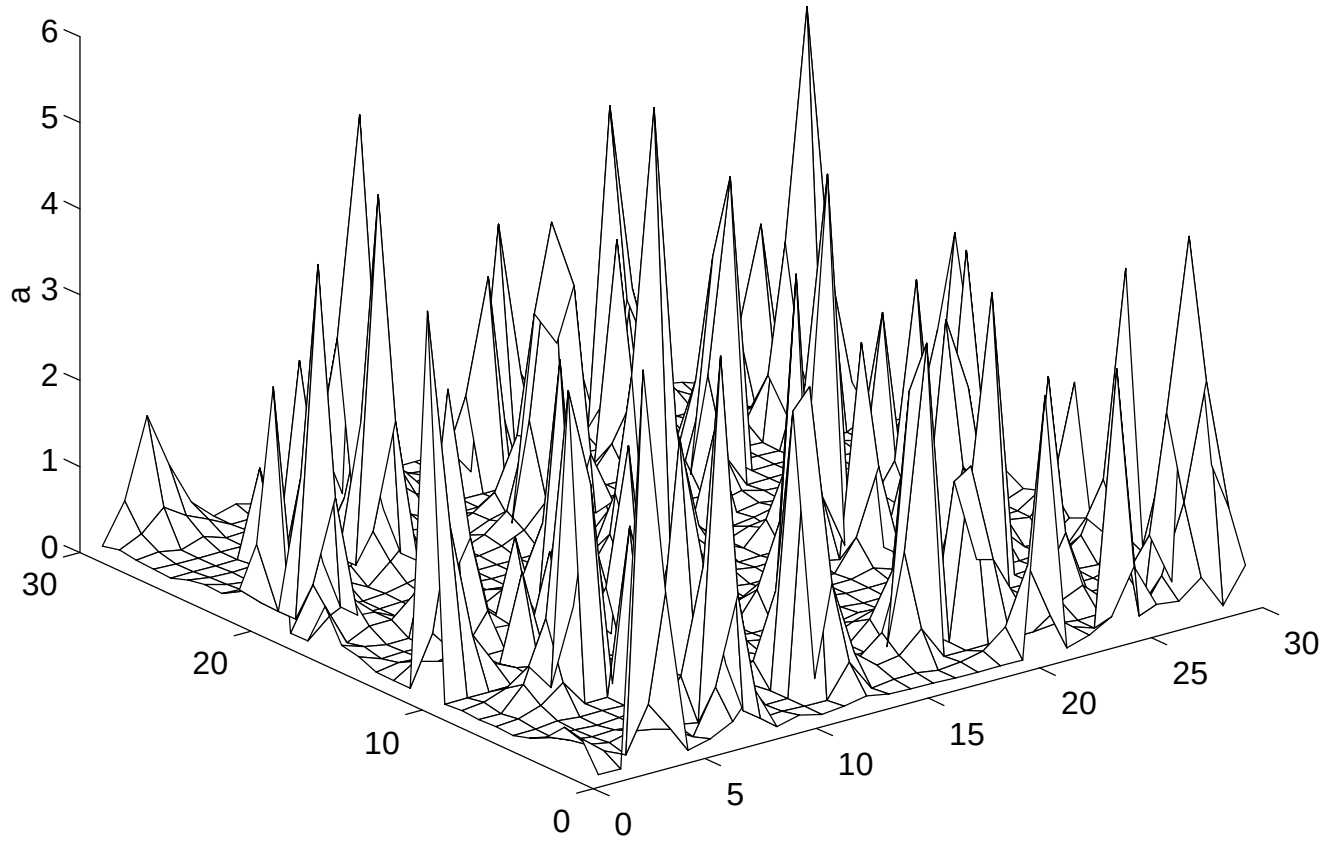

Fig. 1(d)

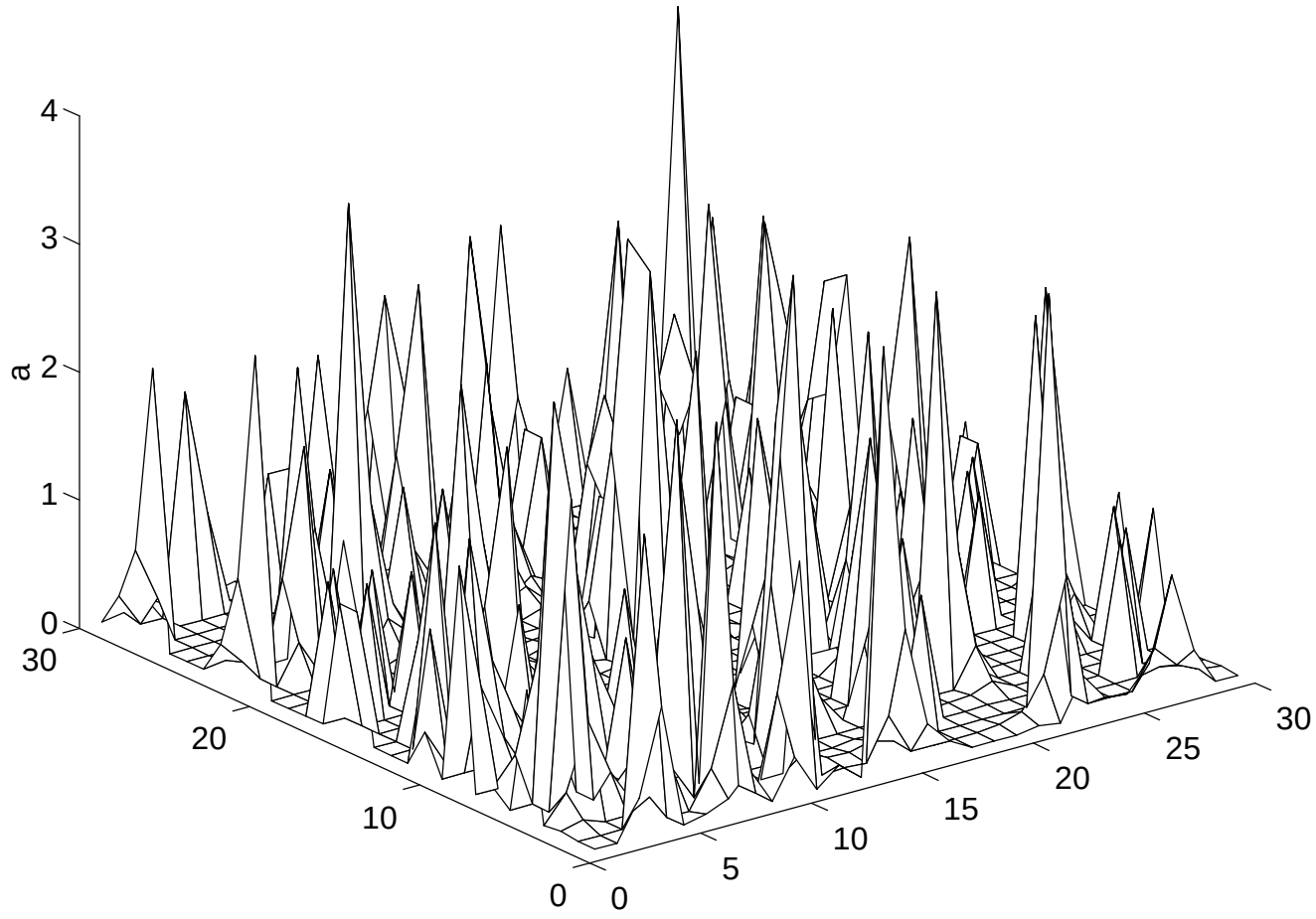

Fig. 2(a)

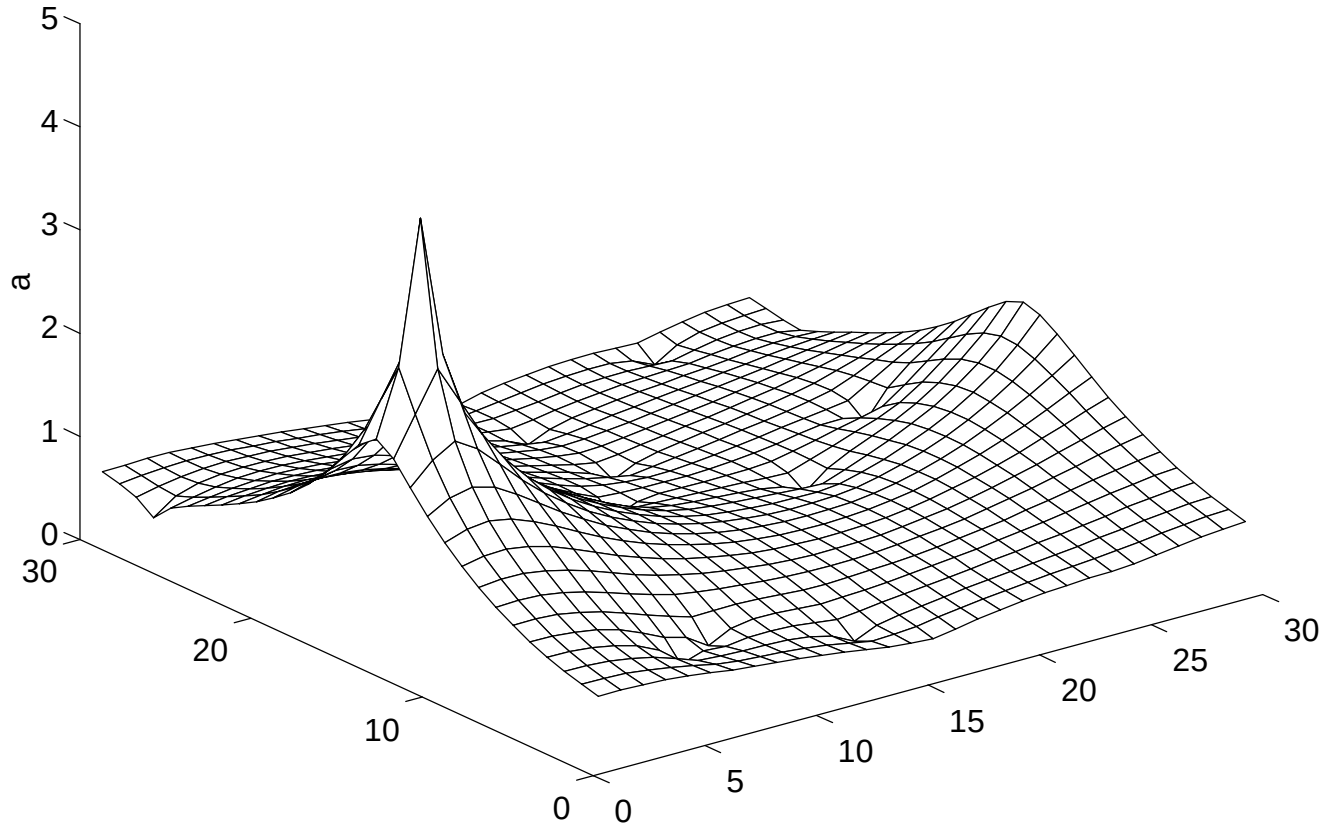

Fig. 2(b)

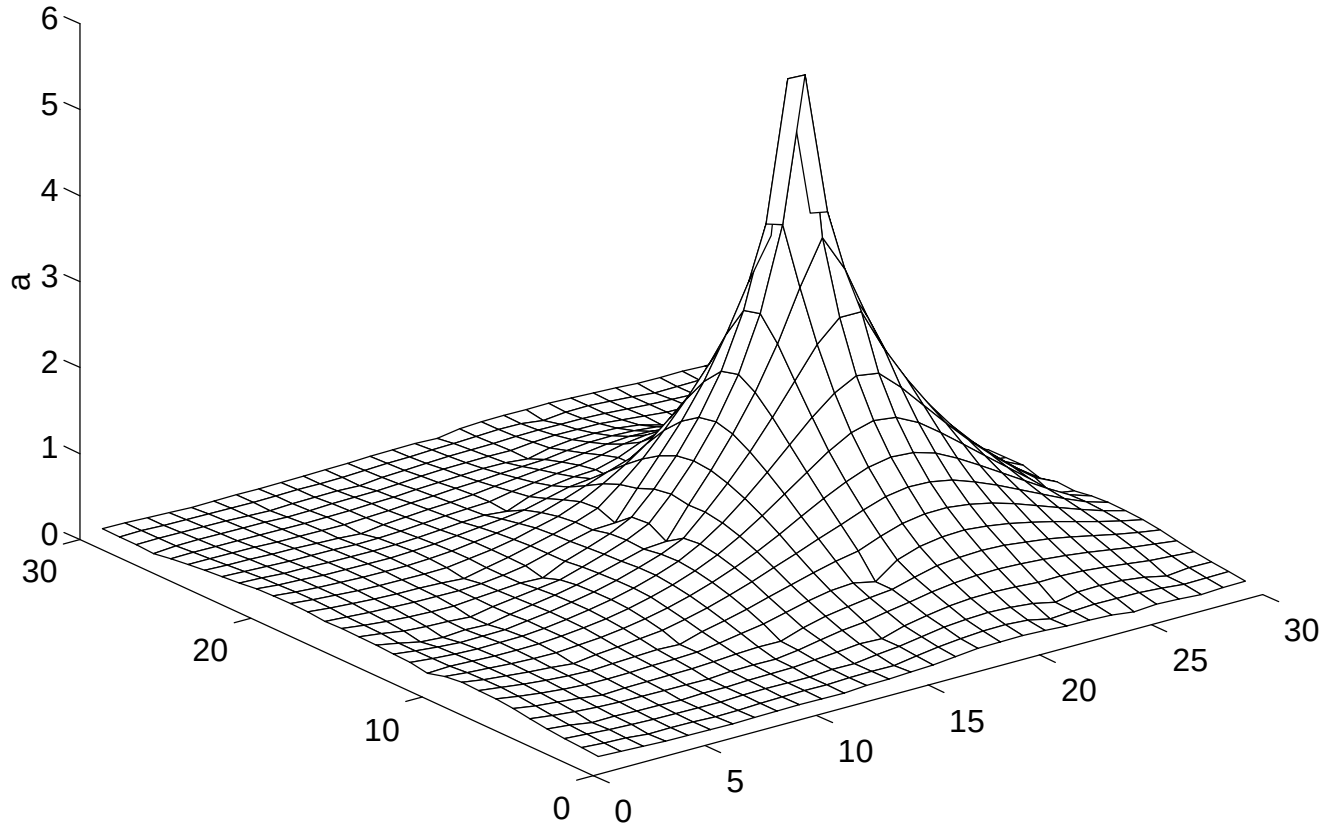

Fig. 2(c)

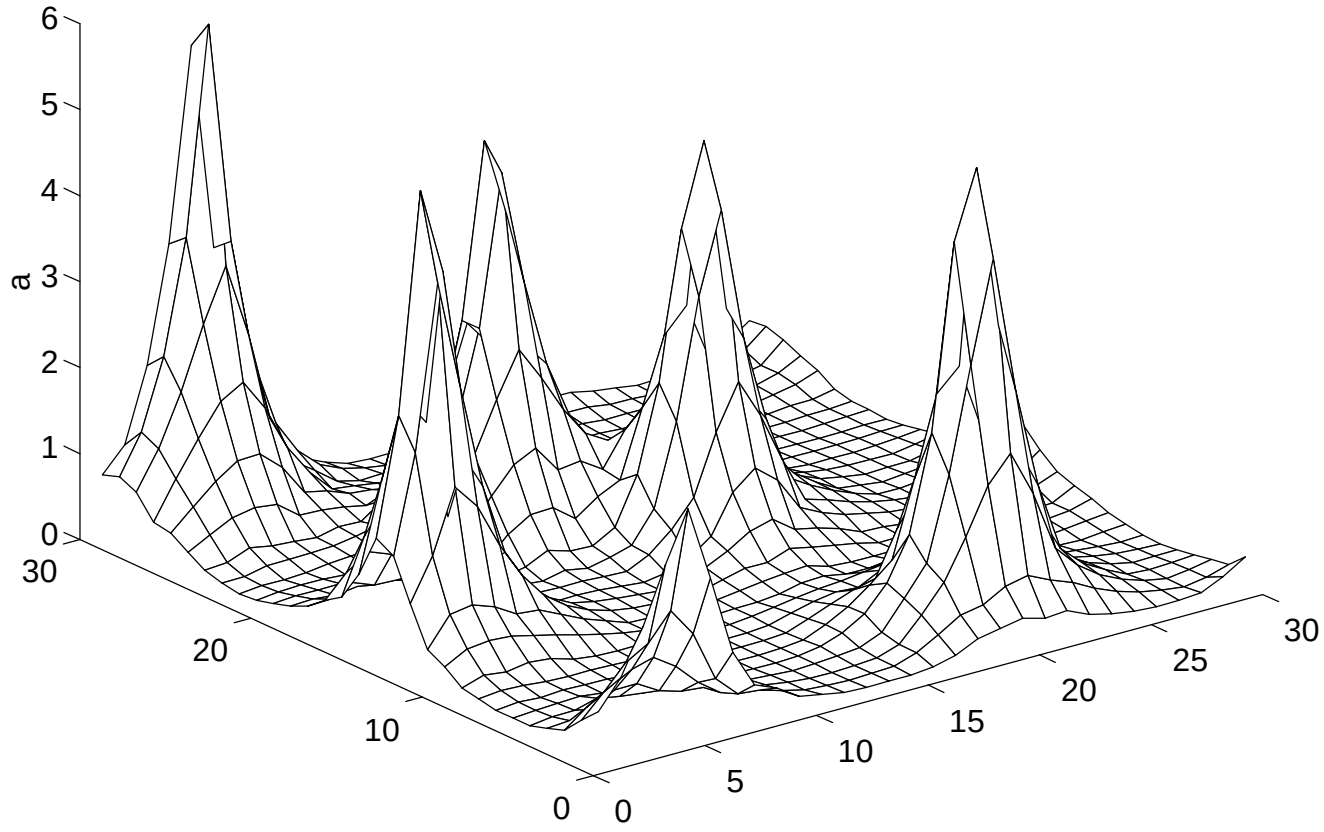

Fig. 2(d)

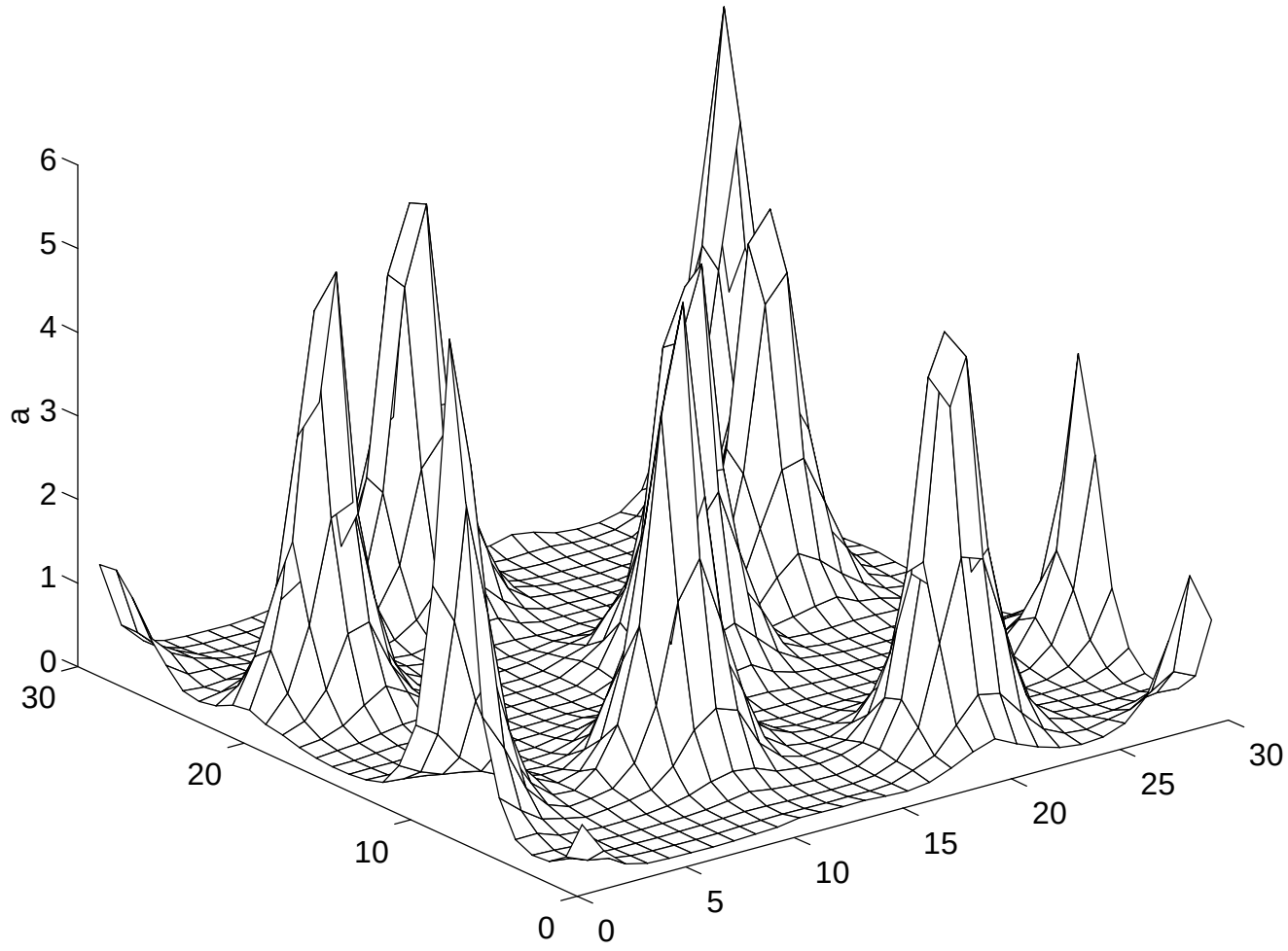

Fig. 3(a)

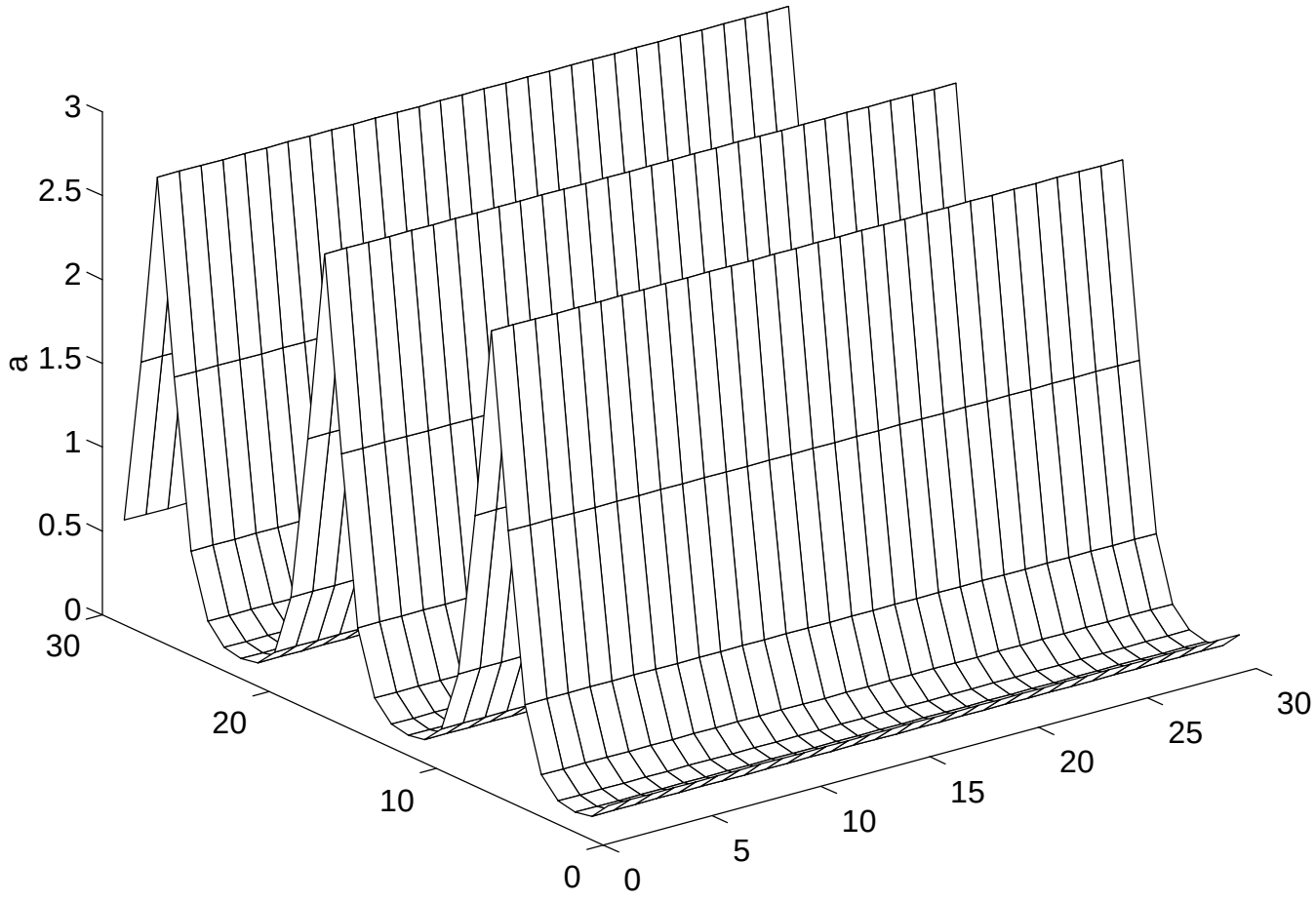

Fig. 3(b)

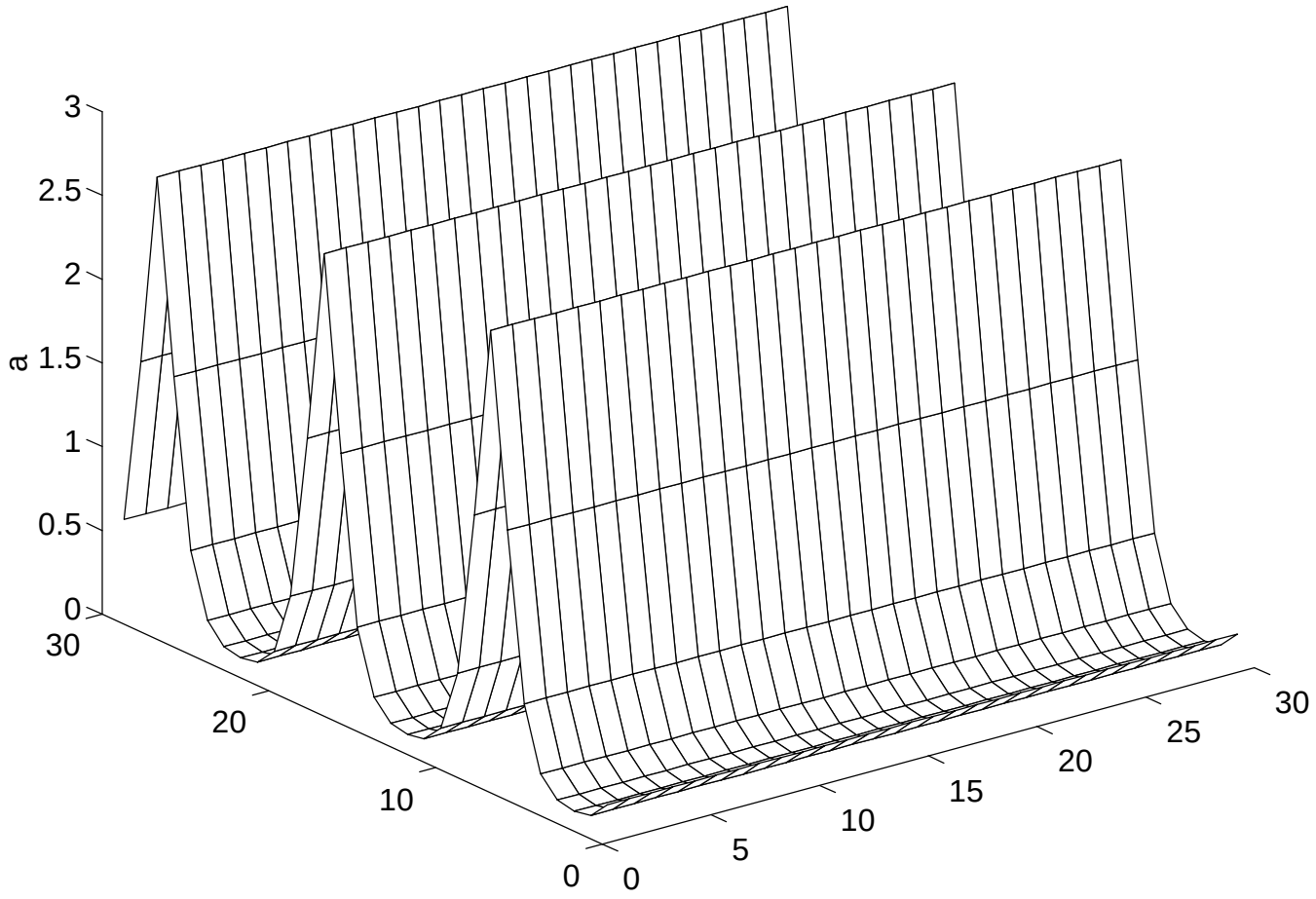

Fig. 3(c)

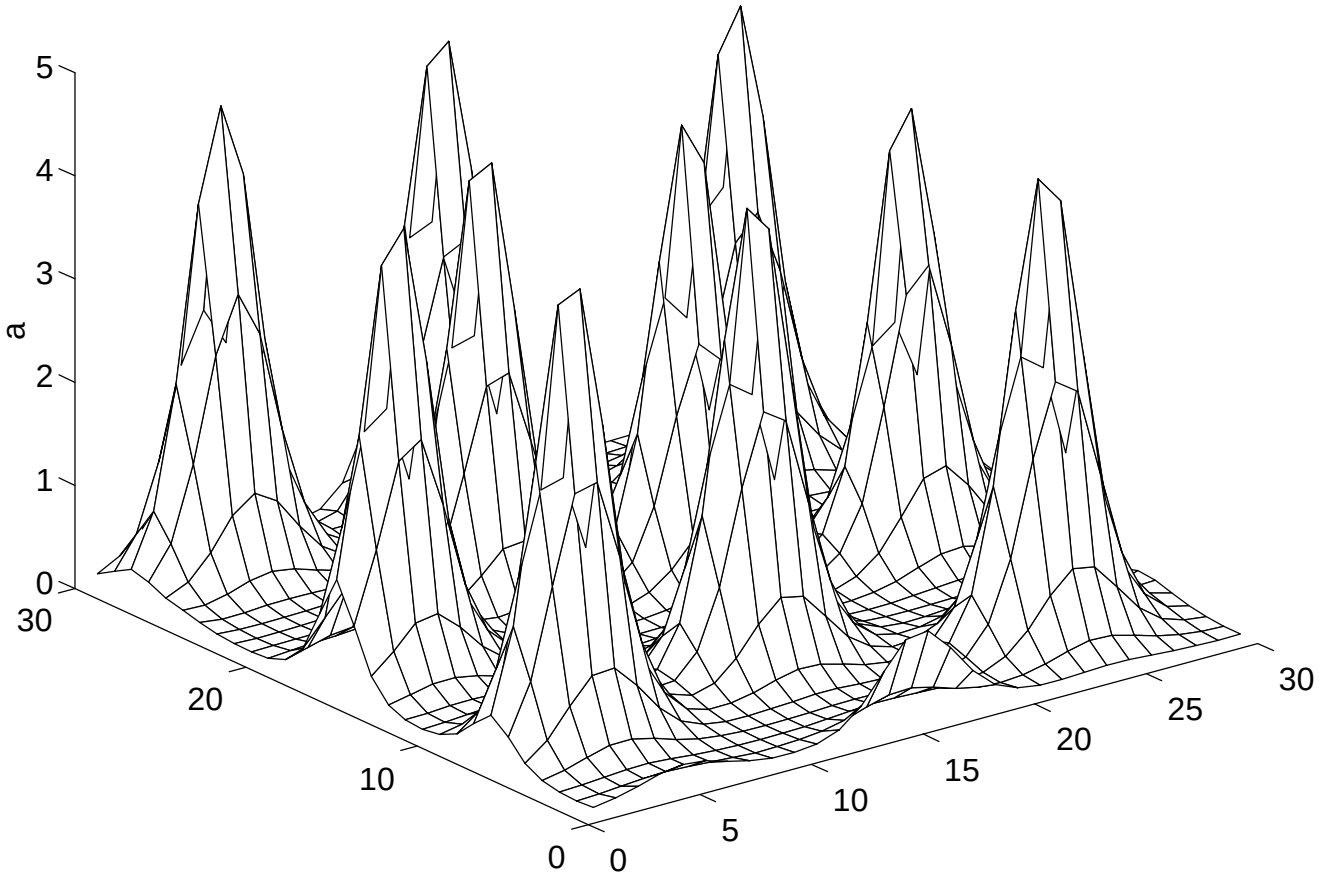

Fig. 4(a)

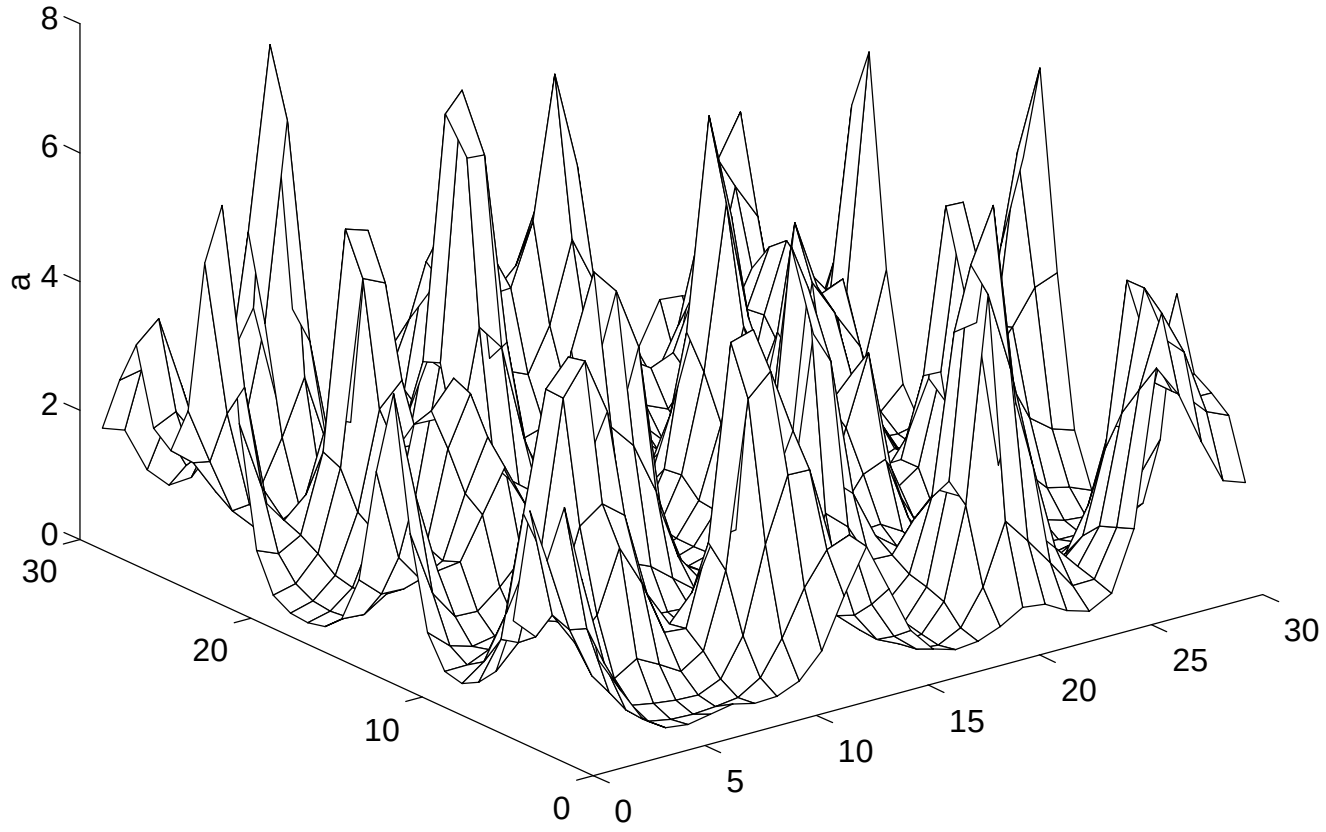

Fig. 4(b)

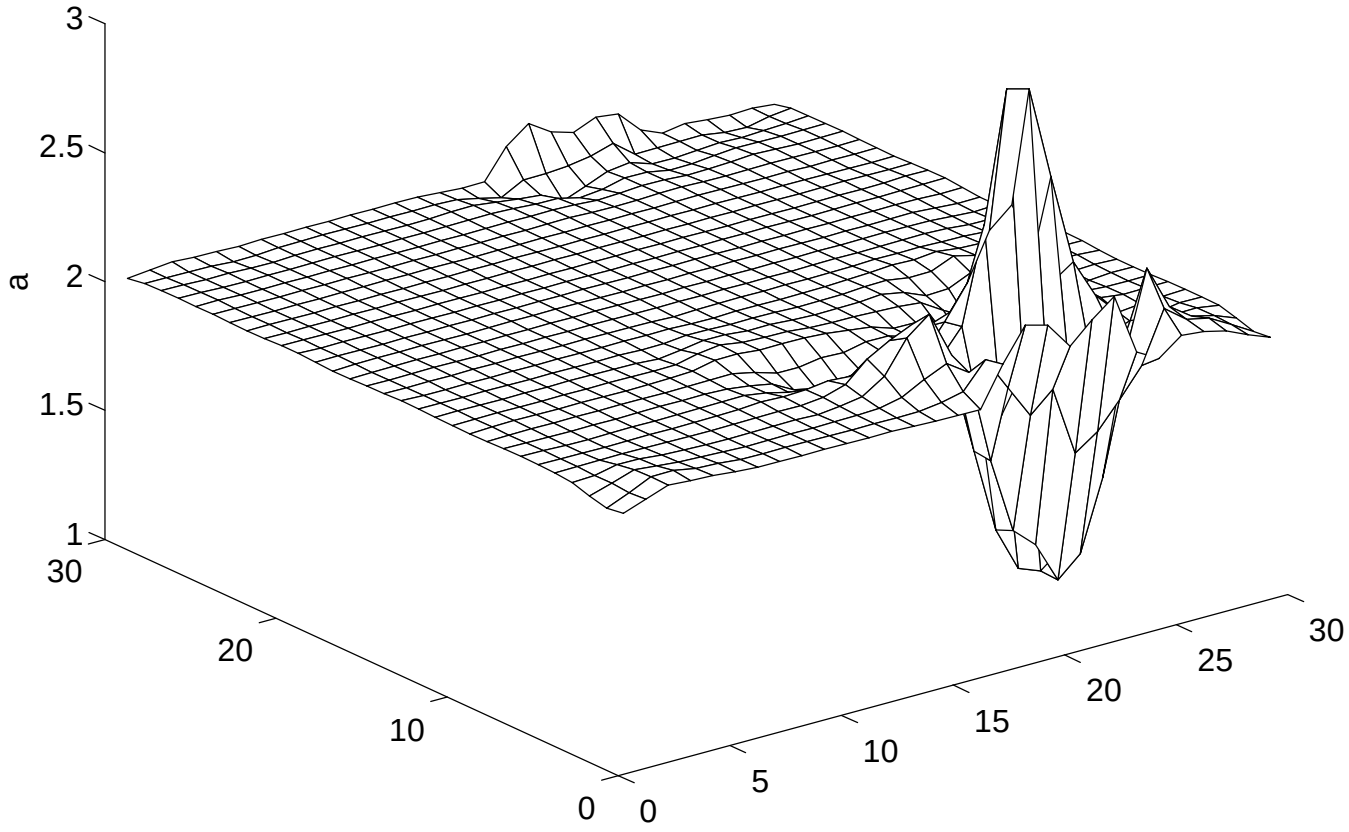

Fig. 4(c)